Master's thesis

NTNU
Norwegian University of Science and Technology

Sigurd Nord Andresen

Planetary Waves over Antarctica

Master's thesis in MTFYMA
January 2022

NTNU
Kunnskap for en bedre verden

Sigurd Nord Andresen

Planetary Waves over Antarctica

Master's thesis in MTFYMA
January 2022

Norwegian University of Science and Technology

NTNU
Kunnskap for en bedre verden

Department of Physics

TFY4900 - Master thesis, physics

Planetary Waves over Antarctica

Author:
Sigurd Nord Andresen

Master thesis, TFY 4900
Supervisor: Patrick Espy
June, 2022

Acknowledgement

First and foremost, I must give a big thanks to my supervisor Patrick Espy for his guidance. He has given me both ideas for the thesis and theoretical explanations along with amusing moments and stories. Lastly, I want to thank my high school physics teacher Christian Foyn for triggering my interest in physics and giving me the motivation to study the field further.

Summary

This thesis investigates a hypothesis proposed by Alan Plumb in 1989 with the object of explaining the mid-winter temperature dip in the upper atmosphere above Antarctica. The basis of the hypothesis lies in the lack of transmission of planetary waves into the upper atmosphere at mid-winter due to the wind reaching the upper limit of the Charney-Drazin criterion. A resulting deceleration of the mesospheric residual circulation and therefore the adiabatic heating occurs. Wave extraction of zonal wavenumber 1 were performed along with wind and temperature from the NAVGEM data for 2016. Disturbances from gravity waves and atmospheric tides were discovered and filtered out in order to isolate the planetary waves. A correlation between the planetary waves and temperature were found, and trends that support Plumbs hypothesis were found as the wave propagation became evanescent as the zonal wind reached maximum values and the following temperature experienced a dip. Anyhow, in the second half of winter, a minor SSW occurred and the erratic winter mesosphere created difficulties regarding a conclusion related to Plumbs hypothesis.

Sammendrag

Denne oppgaven undersøker hypotesen lagt frem av Alan Plumb i 1989 med formålet om å forklare nedkjølingen midtvinter i mesosfæren over Antarktis. Fundamentet til denne hypotesen bygger på at de planetarisk bølgene ikke forplanter seg oppover i atmosfæren da vinden når en styrke som går over den øvre grensen til Charney-Drazin kriteriet. Dette resulterer i en oppbremsning av sirkulasjonen som fører til adiabatisk oppvarming av mesosfæren. De planetariske bølgene med bølgenummer en ble isolert fra vindataen sammen med vind- og temperaturmålinger fra NAVGEM for 2016. Forstyrrelser i uthentingen av de planetariske bølgene ble filtrert ut ved å bruke den daglige gjennomsnittlige vindmålingen. Videre ble korrelasjonen mellom temperaturen og planetariske bølger, samt en trend som kan underbygge Plumbs hypotese, fastslått. De planetariske bølgene ble redusert når vinden nådde maksimale verdier samtidig som temperaturen sank. Sent på vinteren over Antarktisk oppstod det en svak SSW, og den uberegnelige vintermesosfæren gjorde det vanskelig å konkludere rundt Plumb sin hypotese.

Table of Contents

List of Figures

List of Tables

1 Introduction

Large scale atmospheric physics can not be controlled in fixed laboratory systems compared to other segments of scientific research. Hence, the standard within this field is based on observations, hypothesis formulating, testing and re-evaluating the hypothesis. The purpose of this thesis is the latter, namely testing and re-evaluating a hypothesis presented in 1989.

The atmospheric circulations regulate the energy transportation between the atmospheric layers. Significant parts of the dynamics contributing to the regulations are wave-like motions spanning from high frequencies to waves with periods over several days, where the latter is the main topic of this thesis. A combination of pressure differences and the coriolis force gives rise to the large-scale atmospheric waves referred to as planetary waves or Rossby waves. Under certain conditions related to the group velocity of the planetary waves and the strength and direction of the zonal wind, waves can propagate vertically. As they propagate vertically, the density of the surrounding air diminishes. Consequently, the atmospheric wave amplitude grows with increasing altitude. When the conditions are no longer met, the planetary waves break and deposit momentum, altering the mean background flow and driving the atmosphere away from radiative equilibrium. The zonal wind is converted to meridional wind due to the momentum deposited and causes a poleward flow which converge towards the pole, sinks and an adiabatic heating occurs. The conditions required are met above a winter pole. Consequently, one would expect a continuously heating coming into winter at the southern hemisphere as at the northern. However, extensive measurements prove that this is not the case (Labitzke 1981).

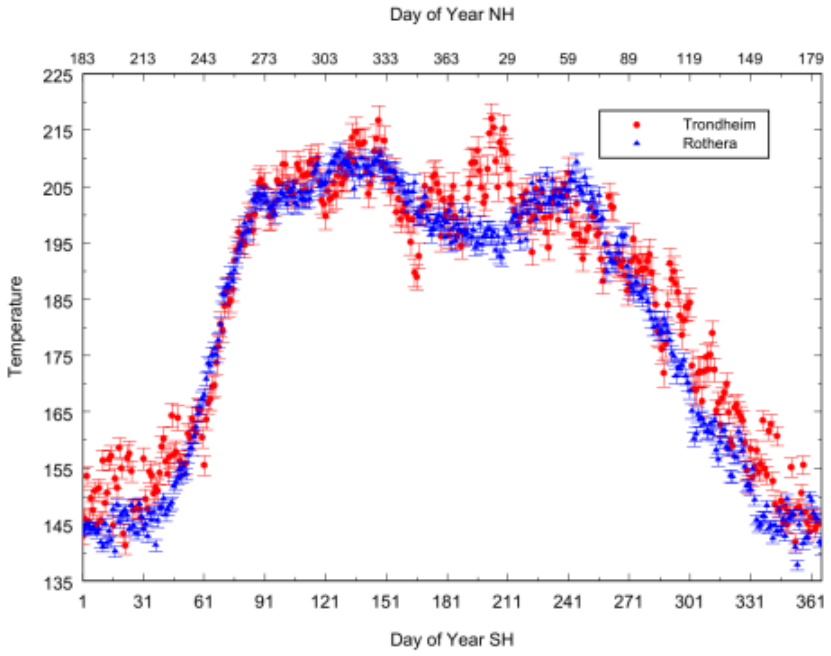

Figure 1: The temperature, measured from meteor radar approximately at 90 km altitude, namely at the mesopause (Espy 2021). The temperature is averaged over 12 years from 2005 to 2017.

In the northern hemisphere, there exists and uneven zonal distribution of land and sea resulting in great pressure differences which gives rise to large-scale planetary waves. Phenomenons such as Sudden Stratospheric Warmings (SSW), where the planetary waves grow strong to such extents that the polar vortex breaks down and changes the stratospheric circulations, are common above the Arctic. At Antarctica, there is an even zonal distribution to land and sea and therefore weaker pressure differences which results in weaker planetary waves. As a result, events like the SSW are rare.

In 1989, Alan Plumb conducted a theoretical research investigating the dynamics behind the mesospheric mid-winter temperature dip at the southern hemisphere, visualized in figure 1. The mid-winter dip is a general weakening of the vortex and a cooling of the upper atmospheric temperature and is observed on the

Antarctic. His proposed explanation has foundation in the zonally symmetric distribution of land and sea at the southern hemisphere. Due to the symmetry, weaker planetary waves are generated and the polar vortex grows stronger. Consequently, the planetary waves are unable to propagate vertically to the mesosphere in the strong mid-winter polar vortex and the adiabatic heating, seen at the northern hemisphere, deceases at mid winter on the southern hemisphere. The purpose of this thesis is to investigate Plumbs hypothesis with the goal to either strengthen or weaken his proposed explanation of this phenomenon.

1.1 Progress of the text

From the outset, a theory section will be presented to lay the foundation needed for explaining the mid-winter cooling over Antarctica. Further, a method section explain the origin of the data set utilized and how the data was handled followed by a section presenting the results from the data analysis. The result section is divided into two sections. One regarding the results in the stratosphere (15 km to 40 km) and one regarding the mesosphere and lower thermosphere (40 km to 95 km). These results will be discussed in the same section followed by a combined discussion weighing the theory up against the results. Lastly, a conclusion will follow.

2 Theory

2.1 Atmospheric structures and characteristics

The atmospheric structure and characteristics lies the foundation for this thesis, and a comprehensive understanding is beneficial for further investigation on the planetary wave activity above Antarctica.

The atmosphere is a composition of gases, with nitrogen and oxygen as the most abundant, surrounding the Earth from the surface, to about 100 km altitude. It determines the energy transfer between the sun and surface and creates motions from the scale of a few meters to earth like dimensions (M. Salby 1995). The latter dimension being, among other, planetary waves which is the focus of this thesis.

For convention, the atmosphere is divided into layers. The boundaries are determined by the change in the temperature gradient as a function of altitude. The troposphere, which is the first layer seen from the earth (figure 2) extends to about 15 km altitude. The dominant source of temperature in the troposphere is surface radiation (Held and Schneider 1999), which diminishes with increasing altitude and leads to a negative temperature gradient with an approximately constant lapse rate. Note that whether the temperature gradient is positive or negative depends on the reference system. For this thesis, increasing altitude is defined as a positive direction. Further, the stratosphere spans from 20 km to 50 km. Due to ozone absorption of solar radiation, the atmosphere heats up with increasing altitude resulting in a positive temperature gradient. In the upper atmosphere, from 50 to 90 km altitude, lies the mesosphere. Due to long wavelength cooling to space from CO_2 results in a negative temperature gradient (Dickinson 1984).

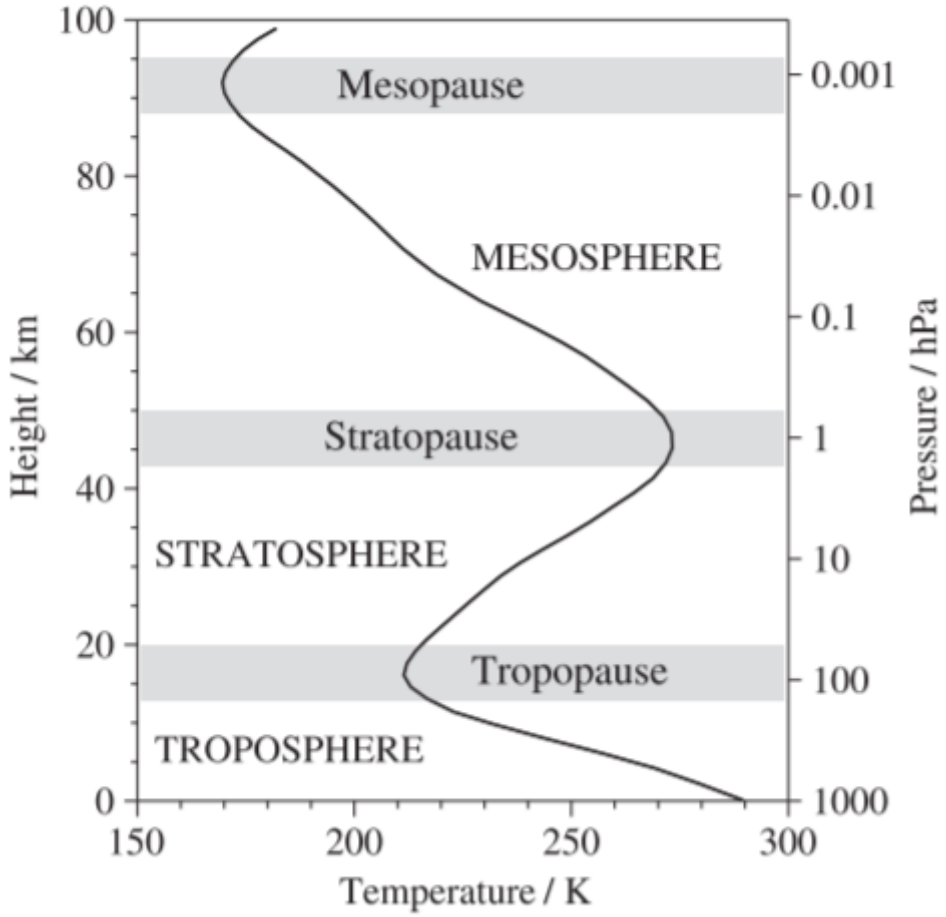

Figure 2: Model of the atmospheric layers and the corresponding height, temperature profile and pressure. The line shows the nature of the temperature gradient. Note that this model is a simplification and can deviate based on season and other factors (Andrews 2010, p. 8).

The hydrostatic balance equation

$$\frac{dp}{dz} = -g\rho \tag{1}$$

is derived on the assumption of an atmosphere at rest and in a static equilibrium (Andrews 2010, p. 22). From equation 1, the pressure at a point in the atmosphere is a function of the mass above this point. Following, the troposphere accounts for 90% of the atmospheric mass followed by the stratosphere which accounts for close to 10%. The mesosphere and further above accounts for approximately 0,1%. Despite the troposphere being the dominant layer in terms of mass, the other layers still serves critical functions and therefore can not be neglected. For instance, short wave heating from O_3 absorption and long wave cooling from CO_2 balances the radiative energy budget, resulting in a middle atmosphere close to being in radiative equilibrium (Andrews 2010, p. 80).

2.2 Navier-Stokes equation of motion

Equation 1 was derived from an atmosphere at rest and in a static equilibrium. As the Earth is spinning, a fluid in a rotating frame is a more accurate description and still mathematically comprehensible. In this section, the Navier-Stokes equation will be derived and modified in order to explain the dynamics of the atmosphere. The deduction will be based on chapter 4 in *An Introduction to Atmospheric Physics* (Andrews 2010).

The atmosphere is treated as a Newtonian fluid and a continuum. Continuums are treated as infinitely many discrete systems and therefor the variables describing the atmospheric behaviour are represented as field variables (M. Salby 1995, p. 322). The general Navier-Stoke equation for a fluid needs to be modified to take Earth's rotation into account. For convention, a fixed coordinate system with respect to the Earth will be used.

The Navier-Stokes equation for a flow of fluids in the inertial frame reads (Andrews 2010, p. 101)

$$\frac{D\mathbf{u}}{Dt} = -\frac{1}{\rho}\nabla p - g\mathbf{k} + \mathbf{F}_{visc}. \tag{2}$$

As the equation defines the motion of a flow, $\mathbf{u}$ represents the flow described. ρ stems from the fluids characteristics and describes the corresponding density while k is the vertical vector defining the direction of the gravitational acceleration g. $\mathbf{F}_{visc}$ represents the viscous force which is the friction of a fluid, and is by definition the difference in horizontal stress on the top and bottom of the discrete system. The stress acting on the system is defined as

$$\tau = \eta\frac{du}{dz}. \tag{3}$$

In order to retrieve the viscous force, the difference in stress is calculated.

$$\delta\mathbf{F}_{visc} = [\tau(z+\delta z) - \tau(z)]\delta x\delta y \approx \frac{\partial\tau}{\partial z}\delta x\delta y\delta z = \frac{\partial\tau}{\partial z}\delta V. \tag{4}$$

The dynamical viscosity is assumed constant which is valid for infinitely small systems. Inserting (3) into (4),

$$\delta\mathbf{F}_{visc} = \eta\frac{d^2u}{dz^2}\delta V. \tag{5}$$

Taking possible variations in every direction into account,

$$\delta\mathbf{F}_{visc} = \delta V\eta(\nabla^2\mathbf{u} + \frac{1}{3}\nabla(\nabla\cdot\mathbf{u})). \tag{6}$$

The resulting viscous force is

$$\mathbf{F}_{visc} = \frac{\delta\mathbf{F}_{visc}}{\delta V}. \tag{7}$$

The resulting Navier-Stokes equation after inserting (6) and (7) into (2) is

$$\frac{D\mathbf{u}}{Dt} = -\frac{1}{\rho}\nabla p - g\mathbf{k} + \eta(\nabla^2\mathbf{u} + \frac{1}{3}\nabla(\nabla\cdot\mathbf{u})). \tag{8}$$

The large-scale atmospheric dynamics are highly dependent of the rotation of the Earth and consequently the equation of motion (8) derived above is incomplete and further modifications of the equation is required.

A rotating reference system fixed to the Earth (R) is designated for convenience. The rotating reference system rotates relative to the inertial reference (I) with an angular velocity $\boldsymbol{\Omega}$. The derivative relationship between a time dependent vector in the two different frames I and R are

$$(\frac{d\boldsymbol{A}}{dt})_I = (\frac{d\boldsymbol{A}}{dt})_R + \boldsymbol{\Omega} \times \boldsymbol{A}. \tag{9}$$

The relationship squared is

$$(\frac{d^2\boldsymbol{A}}{dt^2})_I = (\frac{d^2\boldsymbol{A}}{dt^2})_R + 2\boldsymbol{\Omega} \times (\frac{d\boldsymbol{A}}{dt})_R + \boldsymbol{\Omega} \times (\boldsymbol{\Omega} \times \boldsymbol{A}). \tag{10}$$

The general vector $\boldsymbol{A}(t)$ is set to be a position vector $\boldsymbol{r}$. Double and single time derivative of the position vector provide the acceleration $\boldsymbol{a}$ and velocity $\boldsymbol{u}$ and equation (10) is rewritten as

$$\boldsymbol{a}_I = \boldsymbol{a}_R + 2\boldsymbol{\Omega} \times \boldsymbol{u}_R + \boldsymbol{\Omega} \times (\boldsymbol{\Omega} \times \boldsymbol{r}). \tag{11}$$

Inserting (11) into (8) results in the equation

$$\frac{D\boldsymbol{u}}{Dt} = -\frac{1}{\rho}\nabla p - 2\boldsymbol{\Omega} \times \boldsymbol{u} - \boldsymbol{\Omega} \times (\boldsymbol{\Omega}\times) - g\boldsymbol{k} + F_{visc} \tag{12}$$

which is the Navier-Stokes equation for a fluid in a rotating frame.

2.3 The Fast Fourier transforms

The project report written on "Planetary Waves over Antarctica" concluded that atmospheric tides might have contaminated the planetary wave plots. To verify this conclusion, the Fast Fourier transform is a productive way. The Fast Fourier transform (FFT) is an efficient computational method of the Discrete Fourier transform (DFT). The difference is that for fourier transforming of N data points, the DFT requires N^2 computing operations while the FFT requires $NlogN$ operationsyou (Cooley et al. 1969).

The definition of the DFT is

$$A_r = \sum_{k=0}^{N-1} X_k exp(-2\pi jrk/N), \quad r = 0, ..., N-1 \tag{13}$$

where A_r is the rth coefficient of the DFT and X_k is the value of the function at a discrete time (Cochran et al. 1967)). Effectively, the DFT decomposes a complex signal and returns the frequencies present in the signal. In this thesis, the DFT is utilized to display the waves present in the period domain.

2.4 Planetary waves

For further investigation regarding the research question (section 1), a comprehensive understanding of how planetary waves form is essential. In order to explain how the breaking of planetary waves might effect a mid winter stratospheric cooling, this subsection elucidates how the waves form, propagate and influence the global circulations.

Atmospheric waves are divided into oscillations of the first and second class. Oscillations of the first class include high-frequency buoyancy waves and gravity waves, and can propagate both westward and eastward. Oscillations of the second class are known as planetary waves, often described as Rossby waves. Planetary waves are characterized with thousands of kilometers long wavelengths, periods over several days and can only propagate westwards relative to the background flow.

Simply put, planetary waves are a result of temperature differences and the rotation of the earth. The temperature of the earth is lowest near the poles. Towards the equator, the temperature is warm and the air expands. Looking at a column of air, the vertical pressure is a result of the mass of air particles in

this column. When the air expands, the column grows taller, but with the same amount of air particles. This results in the surface pressure remaining the same, but since the pressure now falls more slowly with altitude due to the taller column, the pressure in the warmer air mass is higher than that in the surrounding cooler air. This results in a force due to the pressure gradient, acting on the air from high pressure to low pressure

$$\vec{F}_{pressure} = \frac{-\nabla p}{\rho}. \tag{14}$$

The rotation contributing to the formation of planetary waves create the Coriolis force. To get a better understanding of the Coriolis force, it is often visualized by a barrel of fluid at the north pole. As the Earth rotates around its own axis in 24 hours at the pole, the fluid in the barrel will look, relative to a similar bucket at the equator, like it is spinning counter clockwise. Air behaves like the fluid in the bucket. As the air is transported from the north pole towards the equator, it will continue to spin counter clockwise. The Coriolis parameter is

$$f = \vec{k} \cdot (\nabla \times \boldsymbol{u}_{earth}) = 2\Omega sin\phi. \tag{15}$$

The Coriolis parameter is maximum at the poles and zero at the equator, which corresponds with the description of a barrel of fluid above.

The difference in pressure and Coriolis force leads to variability in vorticity, which is a key aspect of planetary waves. Vorticity is divided into two categories, planetary and relative vorticity. Carl-Gustav Rossby was able to describe the characteristics of flows in the atmosphere using a single principle. Namely, the conservation of absolute vorticity in a barotropic nondivergent fluid. The conservation of vorticity (16) is derived from the physical property conservation of angular momentum (M. L. Salby 1984).

$$\frac{d(\zeta + f)}{dt} = 0. \tag{16}$$

Planetary vorticity f is the rotation about the axis of the earth

$$f = \vec{k} \cdot (\nabla \times \boldsymbol{u}_{earth}) = 2\Omega sin\phi \tag{17}$$

which is the Coriolis parameter. Relative vorticity ζ is the rotation around a parcel of a fluid's mass centre and is defined as

$$\zeta = \vec{k} \cdot (\nabla \times \boldsymbol{u}) = \frac{\delta v}{\delta x} - \frac{\delta u}{\delta y}. \tag{18}$$

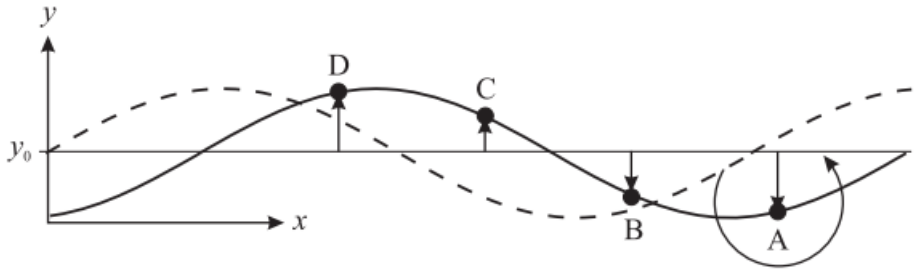

Figure 3: An illustration of how the planetary waves propagate due to conservation of absolute vorticity (16). The figure is from *An Introduction to Atmospheric Physics* (Andrews 2010, p. 136)

Figure (3) illustrates the formation and propagation of planetary waves on the northern hemisphere. A rotating parcel of air is pushed southward due to the pressure force 14. Parcel A in the figure representing the displaced air from high latitudes towards lower latitudes experiences a counter clockwise rotation relative to the new surrounding air. The conservation of vorticity (16) displaces air parcel B due to friction. Further, the rotation of parcel B pushes parcel A back towards higher latitudes, and C toward lower latitudes and so forth. The propagating pattern is westward relative to the mean background flow.

2.5 Gravity waves and atmospheric tides

It is important to mention both gravity waves and atmospheric tides. Both are wave like motions in the atmosphere which complicate planetary-wave research. In order to distinguish the motions and isolate

the planetary waves, in line with the research question, we need to understand how possible disturbances behave.

Gravity waves are high frequency buoyancy waves and arise from density differences. Though internal waves, they form similarly to an ocean wave, where the water in the wave crest is denser than the surrounding air and tends to fall. The air in a wave trough is less dense than the surrounding air and tends to rise. This mechanism gives a wave-like motions in the atmosphere (Andrews 2010, p. 13). Gravity waves generated in the lower atmosphere can propagate vertically up to the mesosphere with wavelengths from 10 to 1 000km and with periods from about 5 minutes up to a day (Hunsucker 1982).

Atmospheric tides are global oscillations. With periods from 12 to 24 hours, compared to 2-20 days for planetary waves. Although their temporal scales are relatively short, their spatial scales are on the same order as those of planetary waves. Thus, tides are more likely to disturb the planetary wave extraction and needs to be taken into account. Tides occur from different sources, which is how they are classified. For instance, the Moon's gravity gives rise to the small amplitude lunar atmospheric tide, while the atmospheric absorption of solar radiation creates the larger solar tides (Hagan 1996). Thermal tides are formed in the Stratosphere due to absorption of solar UV by ozone. As they propagate vertically, the amplitude increases exponentially as the density decreases with altitude (Liu et al. 2010).

2.6 Charney-Drazin criterion

An important property of the mesospheric heating is the Charney-Drazin criterion. It determines the planetary wave filtering and the residual current heating the winter mesosphere. The criterion also lies the foundation for Plumbs hypothesis which this thesis investigates. The theory presented regarding this criterion is written with reference to *Propagation of Planetary-Scale Disturbances from the Lower into the Upper Atmosphere* (Charney and Drazin 1961) and *An Introduction to Atmospheric Physics* (Andrews 2010).

In order to make use of approximations to simplify later on, one must determine the characteristics of planetary waves. For such a purpose, the Rossby number is utilized.

$$\frac{u\frac{\delta u}{\delta x}}{fv} \sim \frac{\frac{U^2}{L}}{fU} = \frac{U}{fL} \equiv Ro \tag{19}$$

The Rossby number is dimensionless and defines the magnitude of horizontal flow relative to the influence of the coriolis force upon the respective flow. A large Rossby number ($Ro >> 1$) indicates that the coriolis force can be neglected. A small Rossby number ($Ro << 1$) indicates a large coriolis force. Planetary waves occur on large horizontal scales L with low frequencies (Andrews 2010, p. 133) and the resulting Rossby number is small. Consequently, the planetary waves are a quasi-geostrophic flow and the geostrophic approximation is valid.

In figure (a)4, a geostrophic flow is visualized and mathematically it is expressed as

$$u \approx u_g = -\frac{\delta\psi}{\delta y}, v \approx v_g = \frac{\delta\psi}{\delta x}. \tag{20}$$

ψ represents the geostrophic streamfunction and a uniform zonal flow has the velocity vector $\vec{U} = (U, 0, 0)$. Accounting for small disturbances or perturbations, the streamfunction is $\Psi = -Uy + \Psi'$. From (20), the geostrophic velocity vector reads (u_g, v_g, o). Since the flow has been established as quasi-geostrophic, one can utilize the following potential vorticity equation

Making use of the quasi-geostrophic potential vorticity equation

$$D_g q = 0 \tag{21}$$

with

$$q \equiv \zeta + \frac{\delta}{\delta z}(\frac{f_0^2}{N_B^2}\frac{\delta\Psi}{\delta z}) = f_0 + \beta + \frac{\delta^2\Psi}{\delta x^2} + \frac{\delta^2\Psi}{\delta y^2} + \frac{\delta^2\Psi}{\delta z^2} + \frac{\delta}{\delta z}(\frac{f_0^2}{N_B^2}\frac{\delta\Psi}{\delta z}). \tag{22}$$

The quasi-geostrophic vorticity equation (21) linearises to

$$(\frac{\delta}{\delta t} + U\frac{\delta}{\delta x})\mathcal{L}\Psi' + \beta\frac{\delta\Psi'}{\delta x} = 0 \tag{23}$$

resulting in the dispersion relation for planetary waves being

$$\omega = kU - \frac{\beta k}{k^2 + l^2 + \frac{f_0^2 m^2}{N_B^2}}. \tag{24}$$

The zonal phase speed of the waves, defined by linear wave theory reads

$$c = \frac{\omega}{k} = U - \frac{\beta}{k^2 + l^2 + \frac{f_0^2 m^2}{N_B^2}}. \tag{25}$$

β comes from the Beta-plane approximation which assumes linear difference in coriolis force with latitude and is defined, with a representing the radius of the earth, as

$$\beta = \frac{2\Omega \cos \phi_0}{a}. \tag{26}$$

In section 2.4, it was established that planetary waves can only propagate westward relative to the background . In fact, this condition is mathematically proven in the calculations above. β is always positive as $\cos \phi_0$ spans from $-\frac{\pi}{2}$ to $\frac{\pi}{2}$. As a result, planetary waves always satisfies $U - c > 0$. For the waves to propagate vertically, it is required that m is real and non-zero. The Charney-Drazin criteria, stating the conditions for planetary waves to propagate vertically, reads

$$0 < U < \frac{\beta}{k^2 + l^2 + \frac{f_0^2}{4N^2H^2}} \equiv U_c. \tag{27}$$

Note that the criterion relates to stationary planetary waves which is the key aspect of this thesis.

2.7 Mesospheric heating at a winter pole

At the winter poles, the pressure gradient points from equator towards the pole resulting in a poleward flow. However, the Coriolis force should turn this flow into the zonal direction. Nevertheless, there is found a wave-driven residual meridional circulation toward the winter pole causing convergent adiabatic heating (Fuller-Rowell 1995). This circulation is called the Brewer-Dobson circulation. The mechanism and driving force of the Brewer-Dobson circulation is the Rossby-wave pump (Butchart 2014).

The Rossby-wave pump is a deviation from the geostrophic balance. The geostrophic balance is a fundamental balance between pressure and Coriolis force which results in a geostrophic flow that is parallel with the isobars (figure 4 (a)). It is defined as

$$-\frac{1}{\rho}\nabla p - 2\vec{w} \times \vec{v}_{rel} = 0. \tag{28}$$

The Rossby wave pump driving the Brewer-Dobson circulation is momentum deposited by Rossby waves, which distorts the geostrophic flow. As planetary waves break and deposit westward momentum, the drag force increases. In figure (c) 4, the drag force is dominant and the flow V is distorted such that the wind is perpendicular to the isobar, pointing from high pressure to low pressure. At a pole-winter, there exists a low pressure and in line with the figure. A poleward flow arises from equator to the winter pole. The flow converges towards the winter pole, sinks and forms a residual meridional circulation causing convergent adiabatic heating (Fuller-Rowell 1995). As discussed in section 2.4, planetary waves have westward momentum relative to the mean background flow, and therefore deposits westward momentum. In order to conserve angular momentum, the pumping drags air upwards close to the equator and sinks at high altitudes.

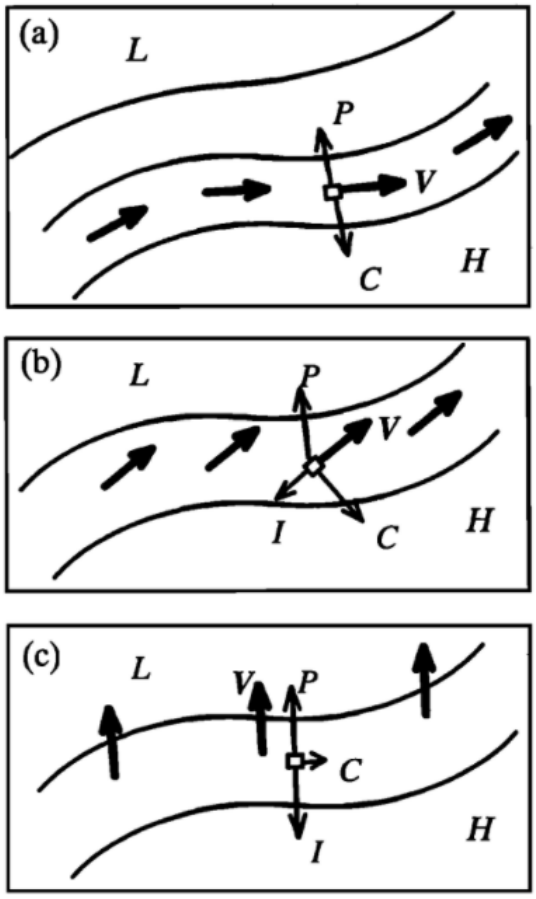

Figure 4: V is the wind, P is the pressure force, C is the Coriolis force, H denotes a high pressure and L a low pressure. (a) is the geostrophic balance. (b) a drag force I is introduced due to the deposit of westward momentum, and distorts the geostrophic flow. (c) drag and pressure is large compared to Coriolis. The figure is extracted from (Fuller-Rowell 1995, p. 26)

At the summer pole, the opposite dynamical phenomenon occurs. The mesosphere above a summer pole is warmer than over equator, due to the solar absorption of ozone and exposure to sunlight (Espy n.d.). This leads to divergent adiabatic cooling in the summer which can be seen in figure 1.

An important factor of the residual circulation is the gravity wave filtering.

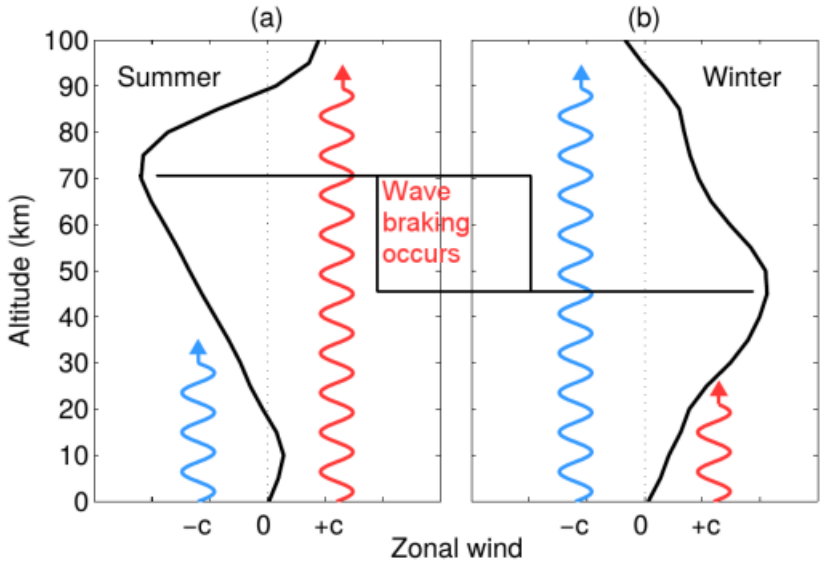

Figure 5: A visualization of the gravity wave filtering. The black line represents the zonal wind as a function of altitude. A negative c (phase velocity) is equivalent with westward propagating gravity waves and positive is equivalent with eastward. The values are extracted at 60°north and the figure is from *Quantifying the influence of the stratosphere on the mesosphere and lower thermosphere* (Wit 2015).

Despite gravity waves being generated in the troposphere, there exists a high density of gravity waves and therefore play a dominant role in the momentum budget of the mesosphere as they break (Smith 1996). From section 2.5, gravity waves can both propagate westward and eastward. With the same dynamical properties as the planetary waves, gravity waves may propagate vertically, break and deposit momentum. For gravity waves to vertically propagate, it is required that wave phase speed is greater than, and in the opposite direction of, the zonal wind. Referring to figure 5, the zonal wind undergoes substantial seasonal variabilities. The seasonal variations in zonal wind is the basis of the gravity wave filtering. A warm summer pole and a cold winter pole generate a temperature gradient resulting in a westward jet on the summer hemisphere and an eastward jet on the winter hemisphere (Schoeberl et al. 1992), which is visualized in figure (5). Ultimately, westward gravity waves cease to propagate in the westward zonal wind in the summer and eastward gravity waves cease to propagate in the eastward zonal wind in the winter. The respective mechanism is also known as the gravity wave filtering.

Planetary waves have the same critical level filtering as the gravity waves, meaning they may not propagate in a wind, in the same direction as the wave, with a speed that exceeds the waves phase speed. In other words, the wind speed must be in the opposite direction relative to the propagating wave. The long periodic planetary waves propagate with a low phase speed, hence the Charney-Drazin criterion (27) is the most limiting case for planetary waves. The gravity waves that do not reach critical levels continue to grow until they overturn and break. This wave breaking is due to the waves perturbing the background temperature gradient to the point that it exceeds the dry adiabatic lapse rate. When this happens, the air motions become unstable and the wave overturns to restore stability (Whiteway et al. 1995).

2.8 Plumbs Hypothesis

In the northern hemisphere stratosphere, there exists a well defined seasonal cycle with low planetary wave activity in the summer, while during winter, they emerge as strong waves. The cycle is interpreted as a sole consequence of the Charney-Drazin criterion (27). The basis for this interpretation, lies in the propagating direction of the zonal wind in the different seasons. Despite consistent observations of a continuously temperature increasing coming into mid-winter on the northern hemisphere, the southern hemisphere stratosphere behaves different. Plumb proposed a hypothesis to explain the differences in his article *On the seasonal cycle of stratospheric planetary waves* (Plumb 1989) which will be the basis for this section.

An indication that the prior interpretation might be inadequate is the stratosphere above the southern hemisphere. Measurements show an increasing planetary wave activity coming into winter, around April and May, before reducing at mid-winter in July and August, and picks up again in September.

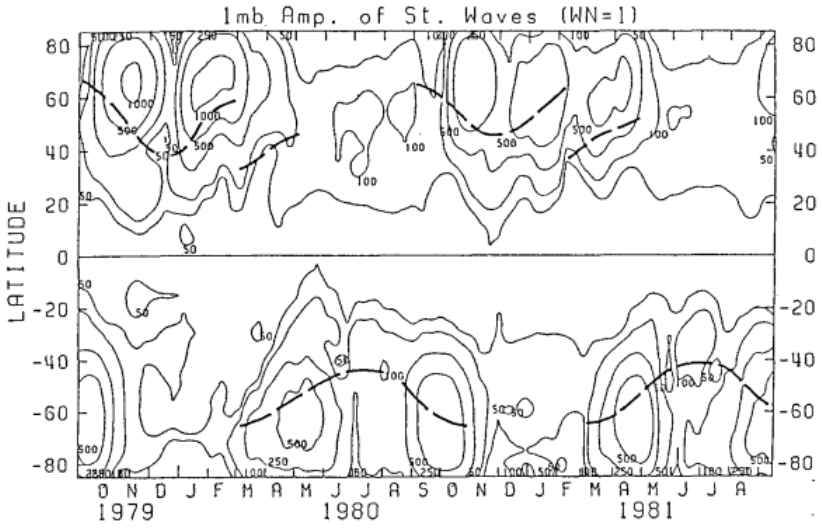

Figure 6: A figure of the amplitude of the monthly-mean wave of zonal wavenumber 1. The amplitude is the geopotential height m, which indicates how high the waves propagate for different months. The time interval is September 1979 to May 1981 and the figure is from Plumb 1989.

.

Plumb suggested that the stratospheric variability between the northern and southern hemisphere stems from the planetary wave source differences in the two hemispheres. Looking at the topography at Antarctica compared to Arctica, the distribution of land and sea is more evenly distributed. An even distribution gives lower local temperature and pressure differences. Following from section (2.4), a smaller pressure gradient leads to weaker planetary waves which results in less westward momentum deposited and a stronger polar vortex. Evidently, less drag force results in a stronger polar vortex which cause the planetary waves to become evanescent due to the upper end of the Charney-Drazin criterion (27) and starve the mesosphere of westward momentum. A resulting slow down of the mesospheric residual circulation and a reduction of the adiabatic heating occurs close to the pole.

Plumb rounds up his paper admitting the proposed hypothesis might be incomplete. In the next sections, a qualitative and quantitative approach will be used in an attempt to strengthen or weaken the hypothesis. Here we will look at a data-driven reanalysis model that gives an accurate picture of the winds and the temperatures in the atmosphere from 15 km altitude to above 90 km. We will quantify the large scale PW amplitudes in this data as a function of height in an effort to see whether the Plumb hypothesis of weakening of upper atmospheric planetary waves during the strong vortex winds at mid-winter results in the temperature dip shown in the climatological temperatures shown in 1.

3 Methods and data

3.1 NAVGEM-data

There are several different approaches to investigate Plumbs hypothesis. In this thesis, the approach is based on planetary wave extraction and looking at the correlation of wind and temperature. The data set provided by Navy Global Environmental Model (NAVGEM) is utilized for this purpose (*Navgem 2.0* n.d.). NAVGEM consists of a grid with spatial resolution of 360° longitude ×180° latitude. The vertical component spans from 15 km altitude to 99 km altitude, with a resolution of one measurement per 2,5 km. The time resolution is one measurement per three hours, in other words 8 measurements per day.

Overall, the NAVGEM data grids have a high resolution. As stated in the introduction, carrying out measurements in the atmosphere is both difficult and expensive, and such a high resolution grid would be close to impossible with actual measurements at every data point. In order to achieve the presented grid, statistical models forecasts data based on actual measurements. A data point sets the benchmark, the model predicts the measurements of nearby grid points. When it reaches a new measurement, the model corrects the predicted data and so forth to fill inn all the data points missing in the grid. The Navier-Stokes equation derived in section 2.2 are crucial for the statistical models prediction as it describes the dynamics of the atmosphere.

3.2 Method

For the purpose of investigating planetary wave activity over Antarctica, in line with this papers research question, the latitude for the investigation was set to 68° south which is the latitude where the Rothera research facility on Antarctica is located. For a given day and a given height, the zonal wind was extracted for each longitude at 12 GTM. In other words, one round around the Earth. A sine wave was fitted and the absolute value of the amplitude of the sine wave was extracted. The amplitude is the strength of the planetary wave. One sine wave is fitted over 360 longitude to extract the planetary waves of zonal wavenumber 1 as seen from figure 7. The reason for using the absolute value of the amplitude, is because a negative amplitude corresponds to a phase shift, which is not relevant for this purpose. The sine wave was also optimized with a phase shift and a constant and the resulting fitted function yields

$$\bar{u} + a \cdot sin(\frac{2\pi}{360} \cdot x + \phi), \tag{29}$$

with x spanning from 0° to 359° longitude. The phase shift parameter makes the plot more correct for phase shifts $\phi \neq \frac{\pi}{n}$. The constant $\bar{u}$ is equivalent to the mean zonal wind.

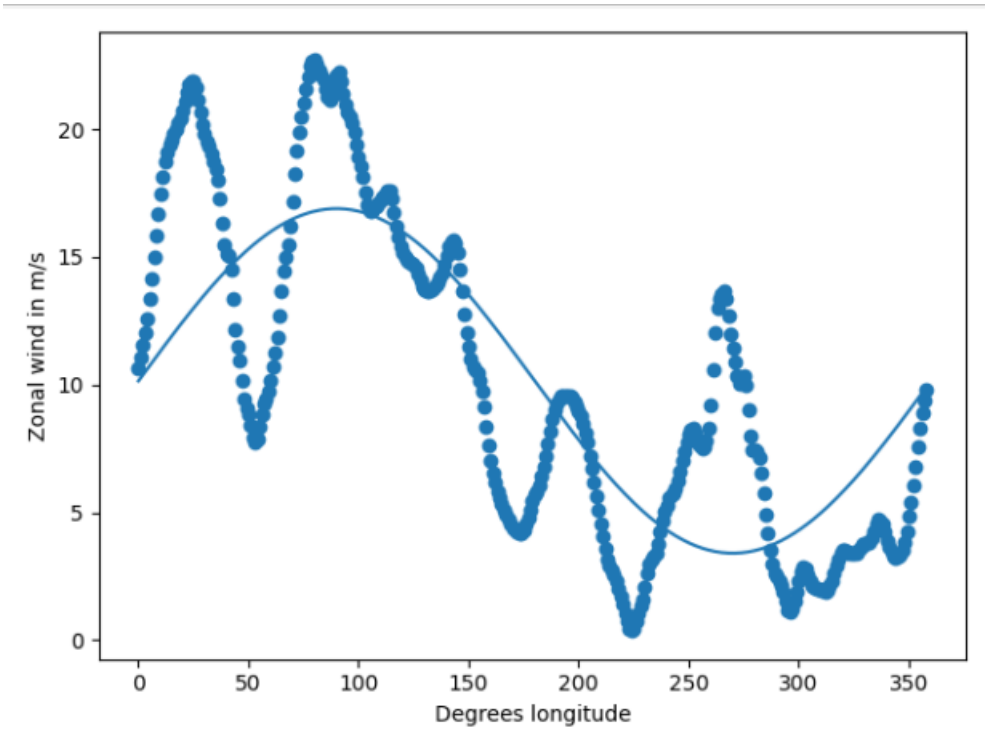

Figure 7: The zonal wind at 18,4km altitude, 68° south as a function of longitude spanning from 0° to 359°. The sine function is fitted for the zonal wind values utilizing equation 29. The sine function fit is the fit of planetary wavenumber 1.

4 Results and discussion

Firstly, this section gives a general overview of the data followed up by results and discussion regarding two subsections. One presenting and discussing the results in the stratosphere (15 km to 40 km altitude) and one regarding the mesosphere and lower thermosphere (40 km to 95 km altitude). Lastly, a combined discussion facilitating a conclusive part is presented. Throughout this chapter, developments in the analysis will be discussed consecutively.

Initially, it was confirmed that the mesosphere above the southern hemisphere experiences a mid-winter cooling compared to the northern hemisphere (figure 1). The research question was whether the hypothesis proposed by Plumb was correct in explaining why the temperature dip occurs. In short, the hypothesis stated that the planetary waves are unable to propagate vertically mid winter as a result of the strong eastward winds, due to the polar vortex, exceeding the upper limit of the Charney-Drazin criterion (27). This again leads to a reduction in westward momentum deposited, which decreases the drag force (figure 4) and the poleward flow diminishes. Evidently, resulting in a deceleration of the mesospheric residual circulation and a reduction of the adiabatic heating occurs above Antarctica (Fuller-Rowell 1995).

Following the method section (3.2), extracting $\bar{u}$ and a from equation 29 at altitudes from 15 km to 95 km for a year, a contour plot for the zonal wind and planetary waves was created.

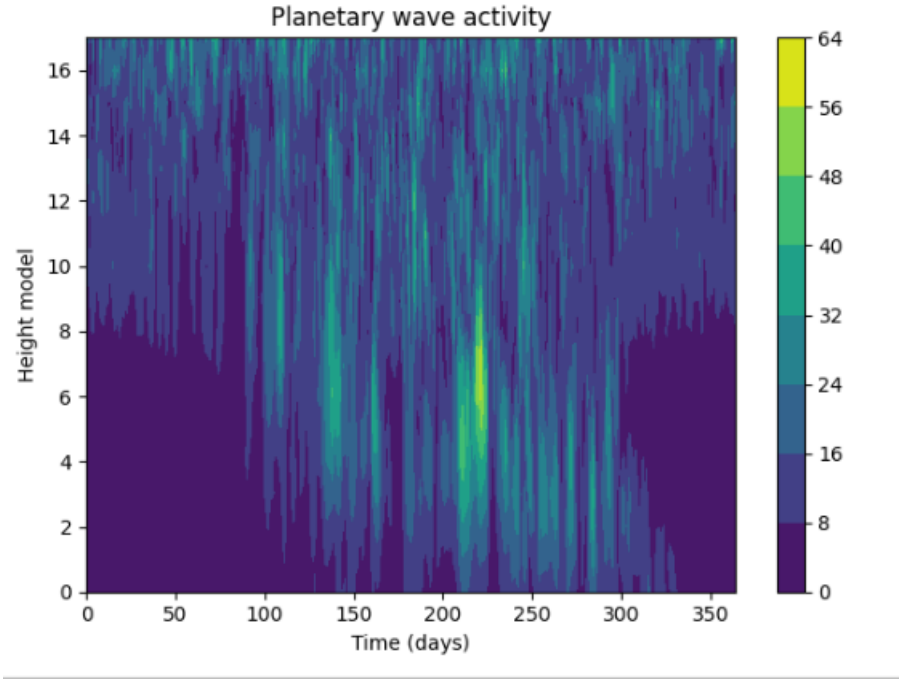

Figure 8: A contour plot of the amplitude of the planetary waves of zonal wavenumber 1, each day for a year at different altitudes. Strength of the amplitude in m/s. Converting tables for height-model to kilometers (2) and days to month (1)

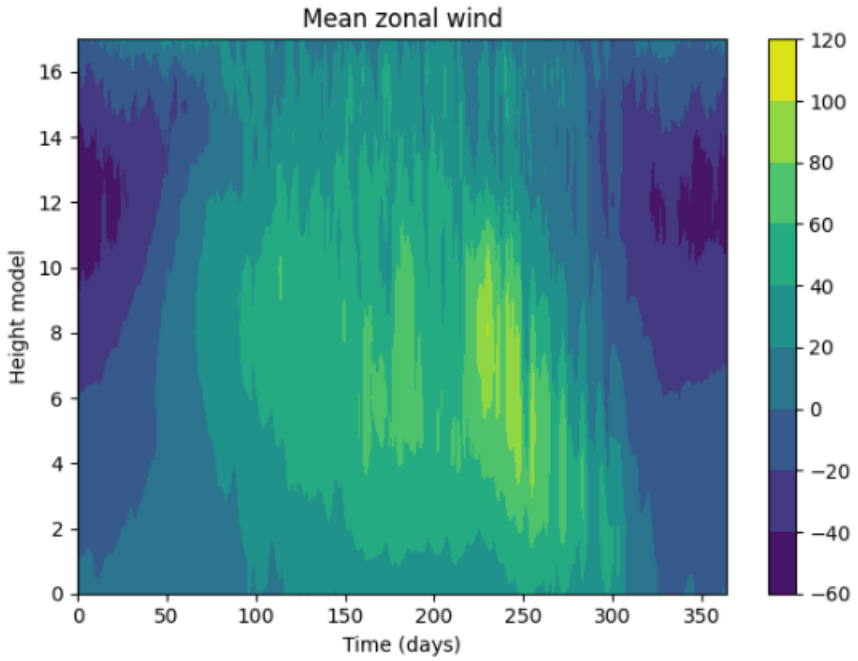

Figure 9: A contour plot of the mean zonal wind, each day for a year at different altitudes. Strength of the wind in m/s. Negative amplitude corresponds with a westward wind. Converting tables for height-model to kilometers (2) and days to month (1)

At mid-summer, day 300 to day 75, there is roughly no planetary wave activity in the the lower atmosphere as shown in figure 8. From the Charney-Drazin criterion 27, planetary waves cease to propagate in a westward relative mean zonal wind. Evidently, the mean zonal wind and planetary wave activity is in line with the theory mid summer below the stratopause (40 km). On the other hand, the mid-summer planetary wave activity above the stratopause is not in line with the Charney-Drazin criterion. The relatively high activity could either be a result of disturbances in the planetary wave extraction or in-situ generated planetary waves.

Entering winter at 50-100 days, the zonal wind turns and picks up along with the planetary waves. At mid winter, day 150-250, the eastward wind reaches its maximum before it diminishes again as summer is approaching around day 300. Further investigations of the correlation between the wind and planetary waves are needed in order to further support Plumbs hypothesis.

4.1 Stratosphere

Atmospheric tides and gravity waves are more likely to disturb the plotting of planetary waves in the upper atmosphere than the lower as the amplitude increases with altitude (Liu et al. 2010). However, atmospheric tides that are generated by water vapour are formed in the troposphere before propagating vertically (Palumbo 1998) which could disturb the plots even in the stratosphere. Gravity waves are formed at lower altitudes. The planetary waves extracted in figure 8 has a sampling frequency of one measurement per day. Instead, utilizing the data with 8 measurements each day, the planetary waves are extracted using the daily averaged zonal wind. Therefore, higher frequency waves, such as gravity waves and atmospheric tides, are more likely to be filtered out.

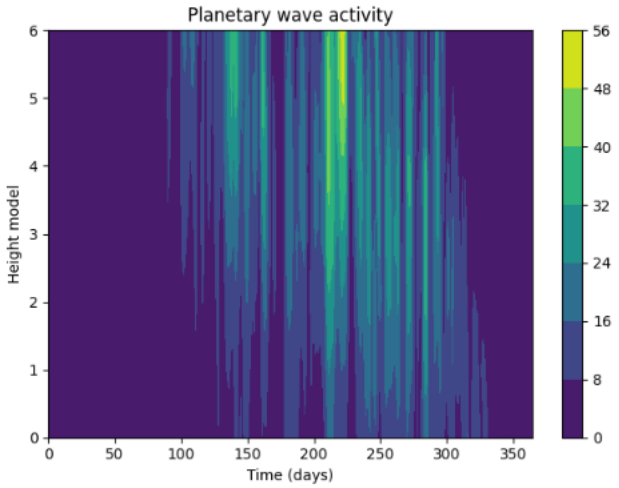

Figure 10: Contour plot of planetary waves in the stratosphere (18 to 40 km altitude) extracted from the daily averaged zonal wind.

The small deviance between figure 8 (height model 0 to 8) and figure 10 indicates that the planetary waves have been extracted with only small disturbances. Atmospheric tides carries heat, and to extend the level of certainty that the plot only contains planetary waves, the temperature as a function of longitude and altitude is visualized for every three hours

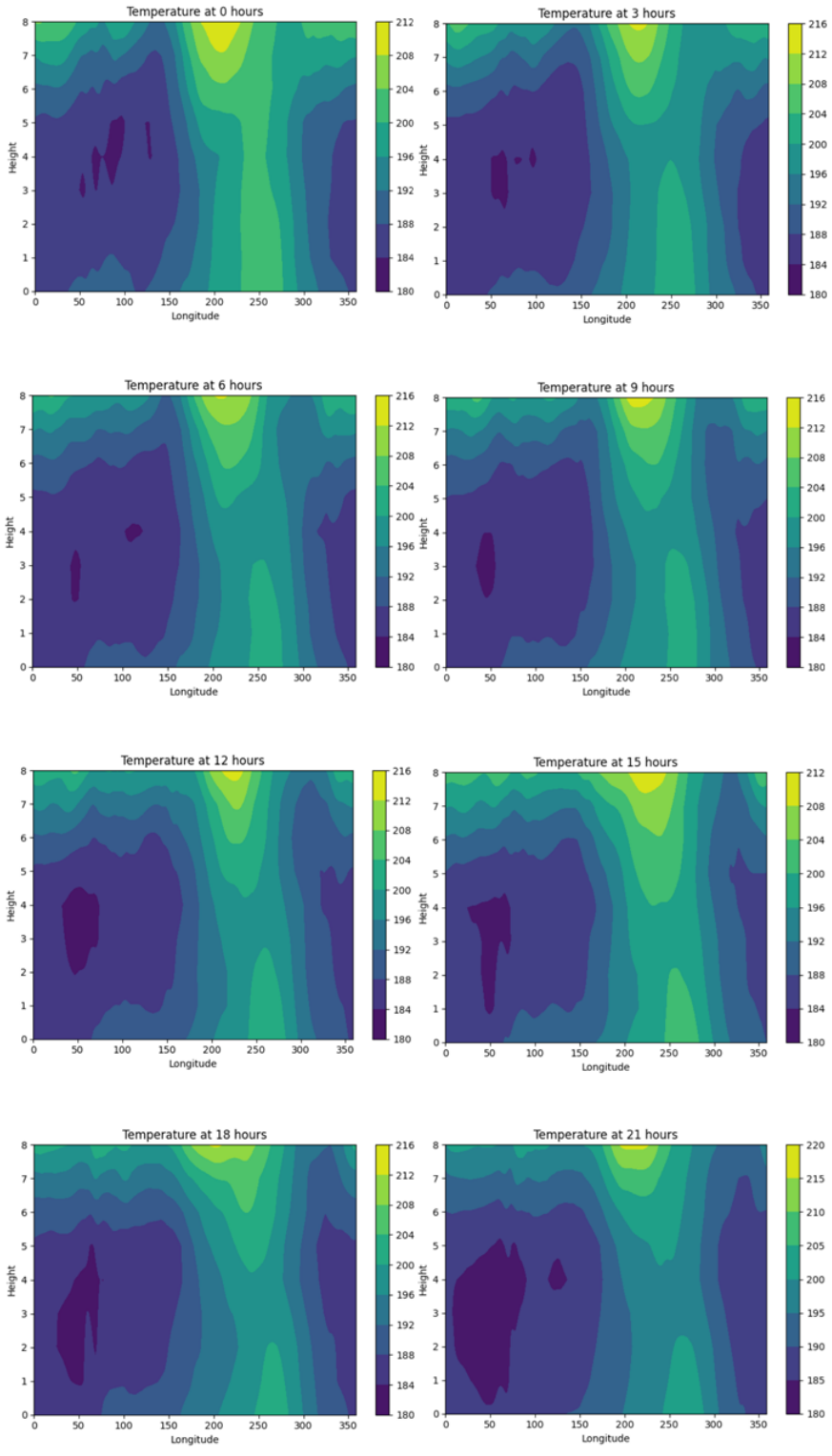

Figure 11: The temperature in Kelvin, at 68°south for every three hours from 18km altitude to 32 km altitude.

A temperature blob moving along the longitudes would be driven by atmospheric tides (Espy 2021). There is no clear movement of temperature, only natural variations, and with more certainty, the wave extraction for the stratosphere only contains planetary waves.

4.2 Mesosphere and lower thermosphere

The deviation in figure 8 from the theory was even greater for the mesosphere and lower thermosphere than for the stratosphere. Both in-situ generated planetary waves, gravity waves and atmospheric tides may be the reason. A quantitative approach to determine whether the reasoning is valid, and the results not being a contradiction to Plumbs hypothesis, would be a fast fourier transform (FFT) (2.3). Performing a FFT before time averaging the data and looking at the frequency domain manifest the periodic waves that are present.

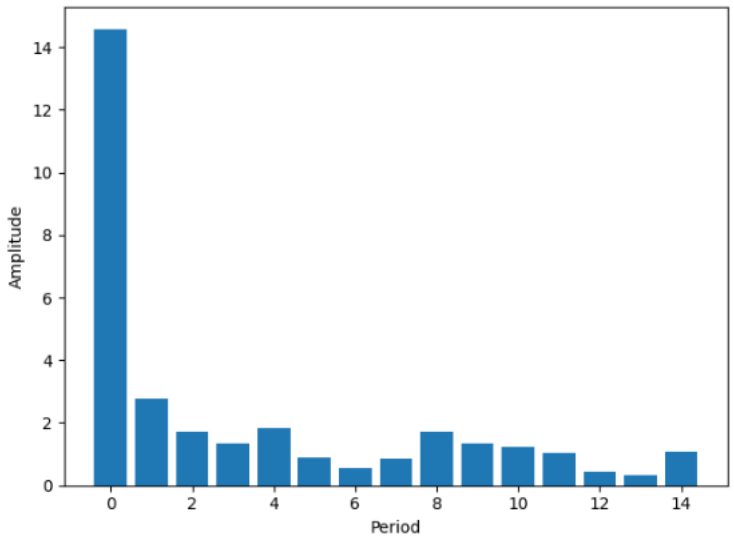

Figure 12: A representation of the periodic waves that are present at 74km altitude in July. The amplitudes represent the magnitude of a periodic wave compared to the other periodicities.

The most common planetary wave periods are 4, 5, 10 and 16 days (Lawrence and Jarvis 2003), while the other periods are likely superpositions of smaller waves. As shown in figure 12, waves with periods below 2 days are the dominant waves in the upper atmosphere at mid-winter. This is a strong indication that the unexpected result from figure 8 is caused by atmospheric tides and gravity waves. To filter out the high frequency (relative to planetary wave frequencies), the planetary waves were extracted from the daily averaged zonal winds as for the stratosphere. Following this procedure, the resulting planetary wave activity in the mesosphere and lower thermosphere is visualized in figure 13.

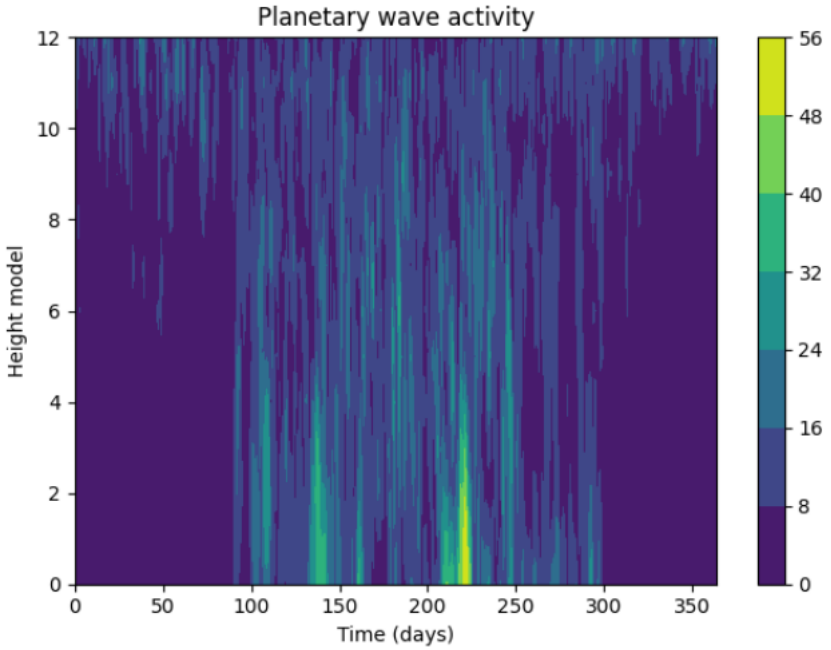

Figure 13: Planetary waves from 40km altitude to 99km altitude with atmospheric tides filtered out.

After filtering out the atmospheric tides, the unexpected high planetary wave activity in the upper atmosphere in figure 8 is significantly reduced in figure 13. Especially in the summer where one would expect zero planetary wave activity. Regardless of the utilization of 8 measurements per day which led to less unexpected activity, there is still some planetary waves in the upper atmosphere in summer. The deviance from the theory is that planetary waves are not able to vertically propagate in the westward wind through height level 8 to 14 (50 km to 79 km) in summer (day 300 to day 50) visualized in figure 9. A plausible explanation for this deviance is in-situ generated planetary waves in the mesosphere and lower thermosphere. In the derivation of the Charney-Drazin criterion (27), a uniform zonal flow $\vec{U} = (U, 0, 0)$ was assumed. In reality, there might be a barotropic/baroclinic instability, meaning there exists a mean flow $\vec{U} = (U_x, U_y, U_z)$ which would alter the vorticity gradient (Sato et al. 2018). As planetary waves are generated from the basis of conservation of absolute vorticity (16), an altered vorticity gradient could give rise to in-situ generated planetary waves in the mesosphere and lower thermosphere. In other words, after the measures taken to filter out atmospheric tides, the unexpected result in figure 13 is probably in-situ generated planetary waves.

For the purpose of this thesis, one must look at the correlation between planetary waves, wind and temperature.

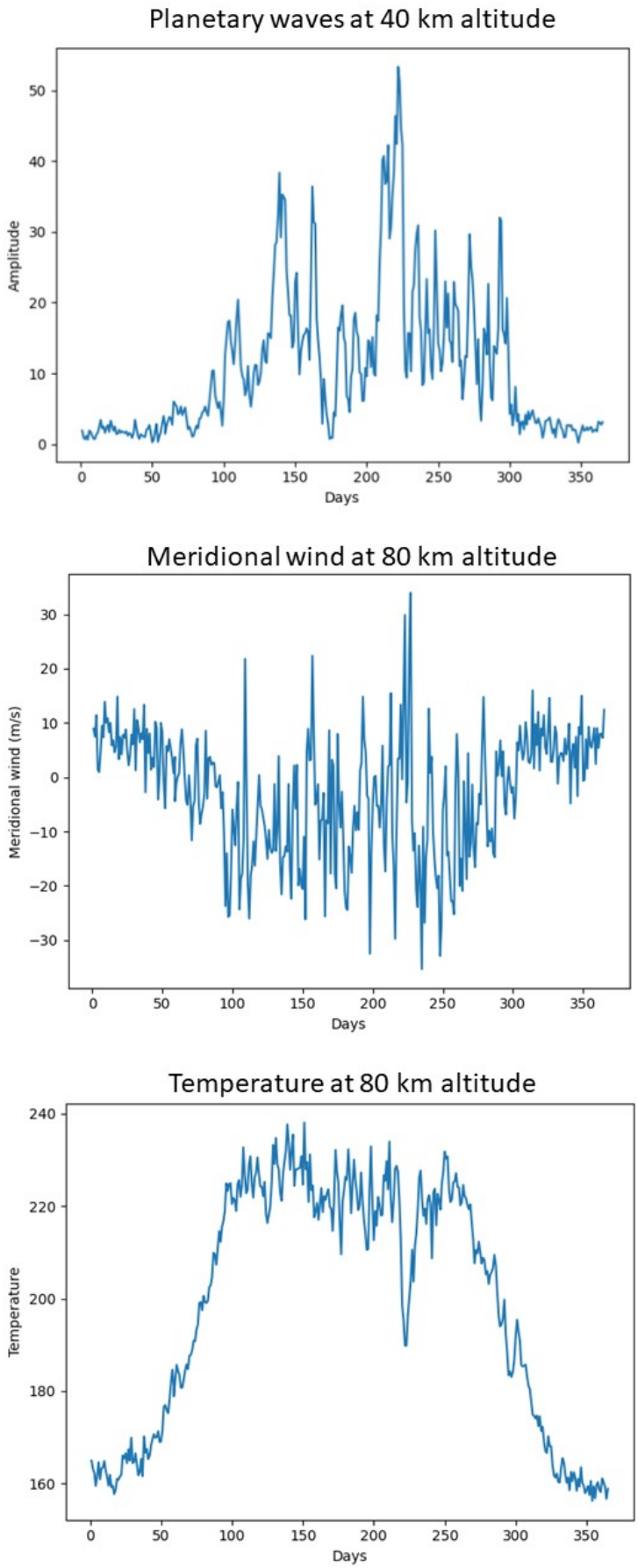

Figure 14: The planetary wave amplitude is in m/s as with the meridional wind. Temperature is given in kelvin.

As planetary waves form at lower altitudes in the winter, they propagate vertically and deposit westward momentum, distort the zonal wind into meridional wind causing a poleward flow (Fuller-Rowell 1995). Therefore, it is reasonable to look at planetary waves at 40 km altitude and temperature and meridional wind at 80 km.

At mid summer, day 250-50, there is hardly any planetary waves leading to less westward momentum deposited and a positive meridional wind. At the southern hemisphere, a positive meridional wind corresponds to a northward flow transporting heat away from the pole which corresponds with the low temperatures in figure 14 in the respective interval.

Approaching winter at day 100, the planetary wave activity increases. As they propagate vertically and break, westward momentum is deposited. As visualized in figure 4, the geostrophic eastward flow is distorted towards the pole. In other words, the zonal wind is converted to negative meridional wind. In accordance with figure 14, increasing planetary wave activity distorts the meridional wind towards the pole which increases the temperature. Mid-winter, between 150 and 200 days, the planetary waves suddenly diminishes and the meridional wind approaches zero amplitude and as a result, the residual current causing convergent adiabatic heating in the mesospheres slows and the temperature experiences a dip. As elaborated in section 2.8, this is the basis for Plumbs proposed explanation to why the temperature profile on the southern hemisphere deviates from the northern hemisphere (figure 1).

Around day 225 in mid august, there is an event that deviates from the trends discussed above and thus need further assessing. There is a sudden spike in planetary wave activity, a spike in positive meridional wind and a drop in temperature. Such an event in the mesosphere could be a result of a sudden stratospheric warming (SSW). SSWs are large and rapid temperature increases at a winter pole due to a breakdown of the stratospheric vortex from a sudden increase in planetary waves above the pole (Butler et al. 2017). In the event of an SSW, the warmer stratosphere leads to a colder mesosphere (Hoffmann et al. 2007).

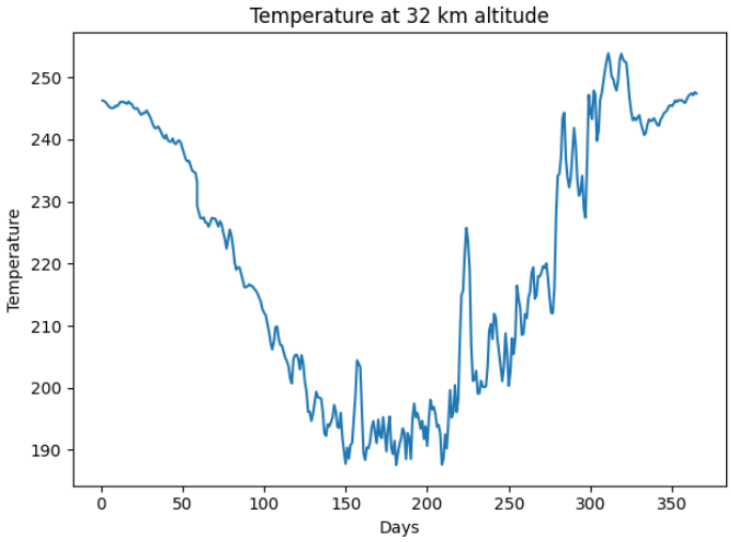

Figure 15: Temperature profile at 32 km altitude above the Rothera Research facility

At day 225, a perfect inverse correlation between the temperature at 32 kilometers altitude (15) and the temperature at 80 kilometers altitude (14) is identified. Consequently, it strengthens the hypothesis that the abnormal event is caused by a minor SSW. The mechanism behind how SSW events lead to mesospheric cooling is a sudden, abnormal peak in planetary wave activity in the stratosphere. Planetary waves propagate westward while gravity waves are both east- and westward. A significant burst of stratospheric planetary waves deposit westward momentum and causes the eastward polar vortex to slow down. This weaker eastward vortex reduces the gravity wave filtering (figure 5). As eastward gravity waves are able to propagate vertically and deposit momentum, the net momentum deposited in the stratosphere reduces and prevents the mesospheric heating mechanism presented in section 2.7.

4.3 Correlation between the zonal winds and planetary waves

A significant correlation between stratospheric temperatures and planetary waves have been established. Nonetheless, to evaluate the hypothesis proposed by Plumb, the correlation between the wind and planetary waves mid-winter needs further investigation. To strengthen the hypothesis, one would expect the planetary wave activity to cut off when the eastward winds reach maximum.

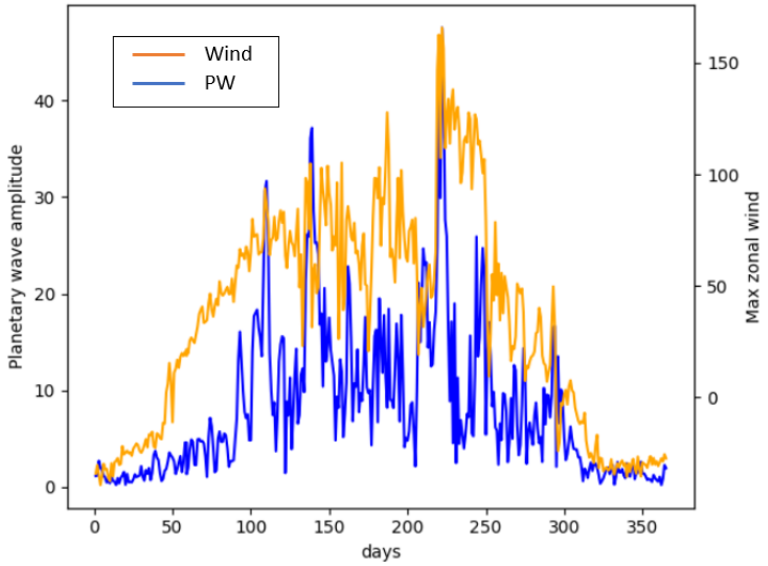

Figure 16: Planetary wave activity extracted at 50 km altitude. The zonal wind is the maximum wind measurement below 50 km altitude.

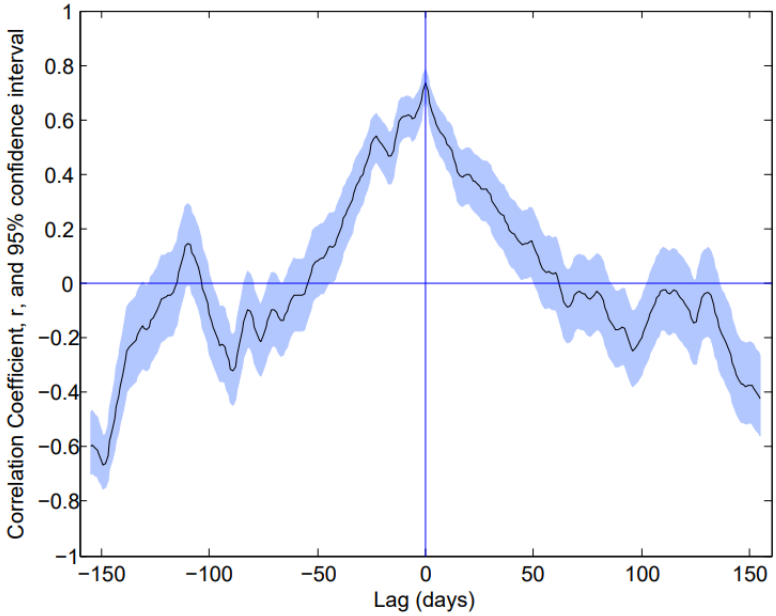

Figure 17: Cross correlation of the period between the zonal wind and planetary waves plotted in figure 16

The cross-correlation is examined with the data visualized in figure 16 as basis. Peaks in the correlation coefficient at negative lag is planetary wave driven winds, while peaks in positive lag is wind driven planetary waves. As visualized in figure 17, there is a strong correlation. Virtually everything has no net shift, meaning that when the winds increase, the planetary waves also increase. This would be the opposite

of what one would expect if the peak in the winds were to decrease the planetary waves at upper levels. It may show that the planetary waves are, in fact, generated by the higher winds, but some other process decreases the winds, and if they are generating the planetary waves, it would also decrease them.

As the atmosphere experiences significant natural variabilities, the plotted values for wind and planetary waves in figure 16 contains a lot of erratic values and there are difficulties in regards of visually determine correlating trends. A general smoothing is beneficial for the purpose of visualizing trends.

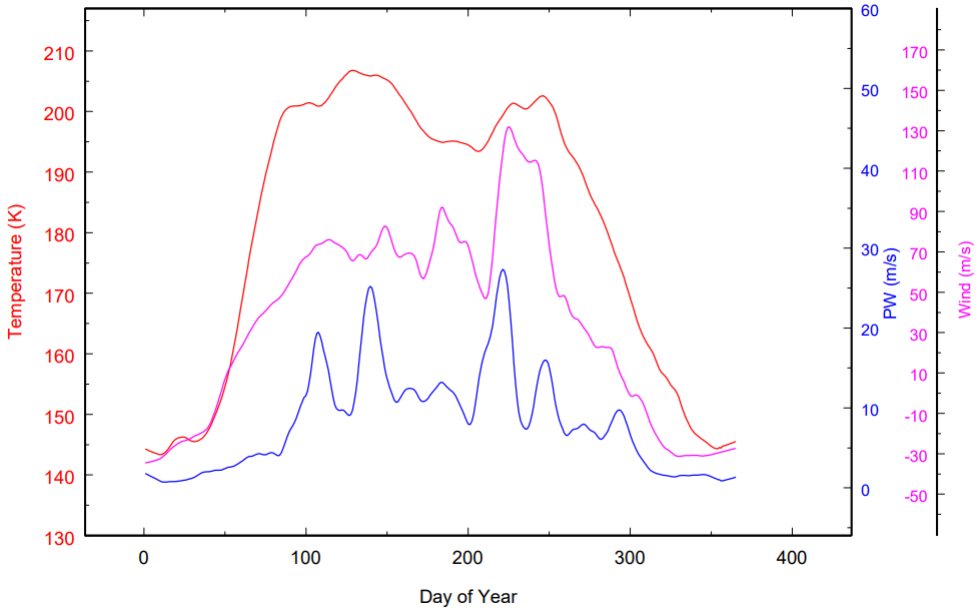

Figure 18: A general smoothing of the planetary wave and zonal wind from figure 16. The temperature is the averaged mesospheric temperature between 2005 and 2017.

Before the abnormal event at day 225, the trend is as Plumb expected. Approaching winter, the zonal wind turns from westward to eastward and the strength increases. Along with the increasing zonal wind, the planetary wave activity picks up with the temperature. Just before day 200, a peak in the zonal wind occurs and the planetary waves experiences a dip. The temperature was averaged over 12 years in order to look at trends. Before day 225, there seems to be a correlation between the wind and wave activity and the temperature. The wind peaks and wave dips occur in the same period as the averaged temperature dip occurs, an indication that the atmosphere behaves like Plumb expected before the SSW.

5 Conclusion

Throughout the years, there has been many scientific studies conducted on the large scale atmospheric dynamics, a field with difficulties related to performing experiments in fixed laboratory systems. A constant challenge with atmospheric physics is measurements, where different methods such as MR radars, falling spheres and radiosondes combined with statistical models to approximate blind spot values are combined in order to achieve a high resolution grid of measurements. In line with these challenges, the article proposing the hypothesis this thesis investigates ends with a statement admitting it might be incomplete.

The research question was whether Plumb was right that the southern hemisphere winds become so strong during winter that they cut off planetary waves in the stratosphere, and this creates the mid-winter cooling. As stated, the mesospheric heating at a winter pole stems from planetary waves propagating vertically as the zonal wind changes from westward to eastward coming into winter. The westward momentum of planetary waves deposit as they break and convert zonal wind to meridional, resulting in a poleward flow, leading to adiabatic heating. Plumb suggested that the topography of Antarctica results in weak planetary waves which enables the polar vortex to strengthen. Due to the Charney-Drazin criterion, the strong polar vortex prevents the planetary waves to propagate into the mesosphere, and the residual current heating the pole mesosphere ceases.

To strengthen Plumbs hypothesis, one would expect the planetary wave activity to cut off as the eastward zonal winds reach maximum. The deviance from the theory in figure 8, with high planetary wave activity all year in the upper atmosphere, were attributable to high frequency waves such as gravity waves and atmospheric tides. After filtering out the high frequencies, the plot corresponded more with what one would expect. The small, but unexpected activity in the upper atmosphere were due to in-situ generated planetary waves. Both in the stratosphere (figure 10) and the mesosphere and lower thermosphere (figure 13) there is hardly any planetary wave activity in the summer. Approaching winter, the zonal wind turns from westward to eastward (figure 9) and as a consequence, the planetary waves start to increase. In figure 18, planetary waves cut off mid-winter (day 150-200) as the wind grows strong which supports Plumbs hypothesis. After day 200, a more irregular pattern occurs, which resembles a SSW, but since a complete reversal of the stratospheric jet did not occur, it is only a minor SSW. During a significant SSW, strong planetary waves break down the polar vortex and the zonal wind turns from eastward to westward. Seen from figure 19, the zonal wind drops rapidly, but does not change direction. Thus, a small scale SSW. Anyhow, such an event has around 4% chance of occurring at the southern hemisphere (Wang et al. 2020). In other words, after day 225, the data is not representative to investigate the atmospheric trends which is a key aspect of Plumbs hypothesis.

Visualized in figure 17, the correlation between the zonal wind and planetary wave were almost perfect which at first sight is a contradiction to Plumb. The abnormal event, on the other hand, contributes to the perfect correlation as both planetary waves and zonal winds peak at day 225. Additionally, the low activity at summer as expected also contributes. In other words, the almost perfect correlation is not necessarily a contradiction.

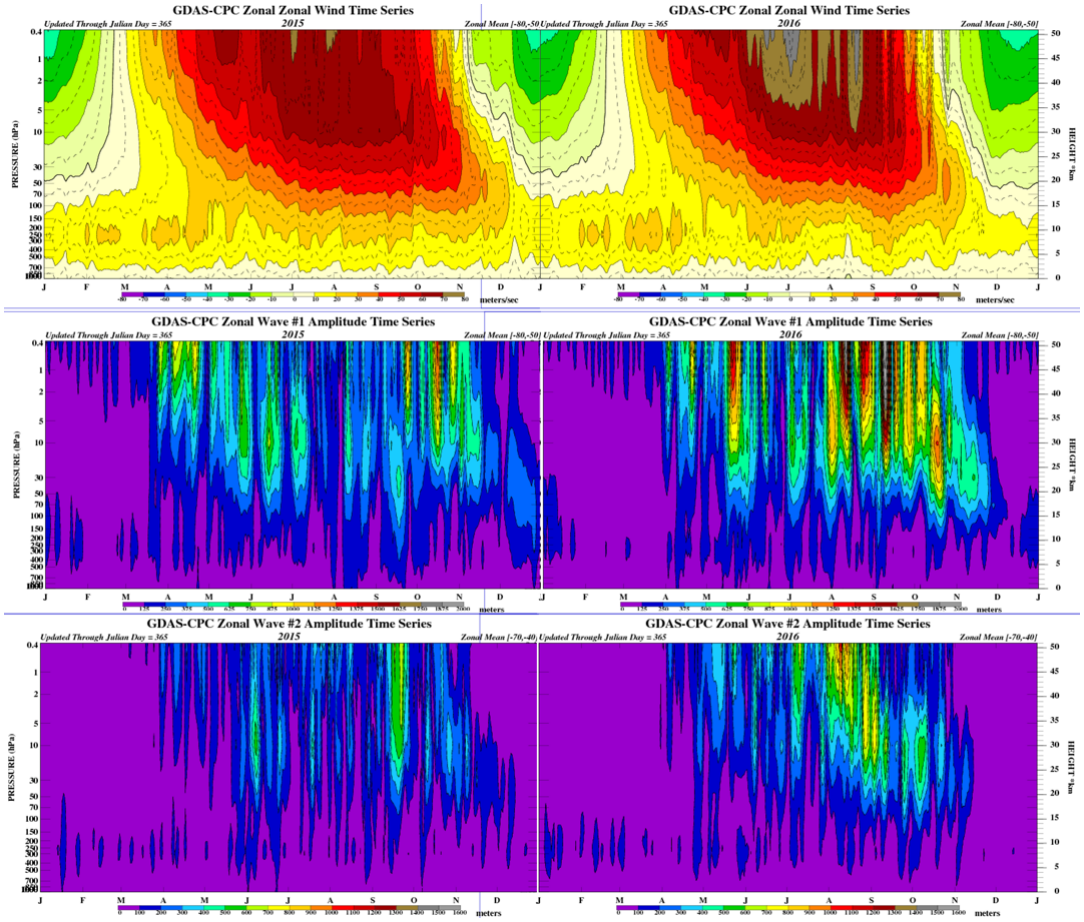

Figure 19: In the upper half, the zonal wind is plotted for 2015 and 2016. At the center, the corresponding planetary wave activity of zonal wave number 1 in 2015 and 2016 is visualized. At the bottom, the planetary wave activity of zonal wavenumber 2 is visualized. The figure is from the Climate Prediction Center (*Stratosphere-Troposhere monitoring* n.d.)

Seen from figure 19, 2016 was a year with a lot of variability and an abnormal event compared to 2015. In 2015, the zonal winds are weaker than in 2016 and steady. The planetary wave activity of zonal wavenumber 1 rapidly declines as the zonal wind peaks between July and August. Along with steady zonal wind and wave 1 drop at mid-winter, 2015 had low wavenumber 2 activity, which is the standard at the southern hemisphere (Espy 2021). 2016 on the other hand had strong and highly erratic zonal wind along with strong activity of wave 2 in late winter. The irregularly strong planetary wave of zonal wavenumber 2 occurs in mid august, and the SSW is likely to occur from the combination of wavenumber 1 and 2. Unfortunately, 2016 was the only available data set from NAVGEM (*Navgem 2.0* n.d.).

In order for a planetary wave to deposit momentum, it has to break or reach a critical value. To break, it needs to propagate vertically and grow unstable. To reach a critical value, it needs to hit a wind that is more westward than its propagation velocity. An extension of the analysis would be to look at the planetary wave differences at different altitude and look at the correlation in the temperature to support Plumbs hypothesis. One must note that gravity waves play the dominant role in the mesospheric momentum budget and therefore it would be relevant perform the same procedure on the gravity waves.

In conclusion, the abnormalities create difficulties to monitor the correlation between zonal wind and planetary waves. It is still not a null result regarding Plumbs hypothesis. The correlation between temperature and planetary waves were established. The general amount of planetary waves was higher in early and late winter corresponding with the mesospheric temperatures. In other words, the temperature dip mid-winter might be a consequence of the reduced transmission of planetary waves as Plumb stated. But in order to draw conclusions, analyzing over several years is paramount as the field of study can not be contained in a laboratory and it is sensitive to natural variations. For further work, the same procedure as done in this thesis with data averaged over several years would remove the variability could confirm or disprove Plumbs hypothesis.

Bibliography

Andrews, David G. (2010). *An Introduction to Atmospheric Physics*. Cambridge University press.

Butchart, Neal (2014). 'The Brewer-Dobson circulation'. In: *Reviews of geophysics* 52.2, pp. 157–184.

Butler, Amy H et al. (2017). 'A sudden stratospheric warming compendium'. In: *Earth System Science Data* 9.1, pp. 63–76.

Charney, J. G. and P. G. Drazin (1961). 'Propagation of planetary-scale disturbances from the lower into the upper atmosphere'. In: *Journal of Geophysical Research (1896-1977)* 66.1, pp. 83–109. DOI: https://doi.org/10.1029/JZ066i001p00083. eprint: https://agupubs.onlinelibrary.wiley.com/doi/pdf/10.1029/JZ066i001p00083. URL: https://agupubs.onlinelibrary.wiley.com/doi/abs/10.1029/JZ066i001p00083.

Cochran, William T et al. (1967). 'What is the fast Fourier transform?' In: *Proceedings of the IEEE* 55.10, pp. 1664–1674.

Cooley, James W, Peter AW Lewis and Peter D Welch (1969). 'The fast Fourier transform and its applications'. In: *IEEE Transactions on Education* 12.1, pp. 27–34.

Dickinson, Robert E (1984). 'Infrared radiative cooling in the mesosphere and lower thermosphere'. In: *Journal of atmospheric and terrestrial physics* 46.11, pp. 995–1008.

Espy, Patrick (2021). personal communication.

— (n.d.). *Thermal Winds*. University lecture. Course FY3201.

Fuller-Rowell, TJ (1995). 'The dynamics of the lower thermosphere'. In: *The Upper Mesosphere and Lower Thermosphere: A Review of Experiment and Theory, Geophys. Monogr. Ser* 87, pp. 23–36.

Hagan, ME (1996). 'Comparative effects of migrating solar sources on tidal signatures in the middle and upper atmosphere'. In: *Journal of Geophysical Research: Atmospheres* 101.D16, pp. 21213–21222.

Held, Isaac M and Tapio Schneider (1999). 'The surface branch of the zonally averaged mass transport circulation in the troposphere'. In: *Journal of the atmospheric sciences* 56.11, pp. 1688–1697.

Hoffmann, P et al. (2007). 'Latitudinal and longitudinal variability of mesospheric winds and temperatures during stratospheric warming events'. In: *Journal of Atmospheric and Solar-Terrestrial Physics* 69.17-18, pp. 2355–2366.

Hunsucker, Robert D (1982). 'Atmospheric gravity waves generated in the high-latitude ionosphere: A review'. In: *Reviews of Geophysics* 20.2, pp. 293–315.

Labitzke, Karin (1981). 'Stratospheric-mesospheric midwinter disturbances: A summary of observed characteristics'. In: *Journal of Geophysical Research: Oceans* 86.C10, pp. 9665–9678.

Lawrence, AR and MJ Jarvis (2003). 'Simultaneous observations of planetary waves from 30 to 220km'. In: *Journal of atmospheric and solar-terrestrial physics* 65.6, pp. 765–777.

Liu, H-L et al. (2010). 'Thermosphere extension of the whole atmosphere community climate model'. In: *Journal of Geophysical Research: Space Physics* 115.A12.

Navgem 2.0 (n.d.). https://www.hycom.org/dataserver/navgem.

Palumbo, A (1998). 'Atmospheric tides'. In: *Journal of atmospheric and solar-terrestrial physics* 60.3, pp. 279–287.

Plumb, R.Alan (1989). 'On the seasonal cycle of stratospheric planetary waves'. eng. In: *Pure and applied geophysics* 130.2-3, pp. 233–242. ISSN: 0033-4553.

Salby, Murry (1995). *Fundamentals of Atmospheric Physics*. Academic Press.

Salby, Murry L (1984). 'Survey of planetary-scale traveling waves: The state of theory and observations'. eng. In: *Reviews of geophysics (1985)* 22.2, pp. 209–236. ISSN: 8755-1209.

Sato, Kaoru, Ryosuke Yasui and Yasunobu Miyoshi (2018). 'The momentum budget in the stratosphere, mesosphere, and lower thermosphere. Part I: Contributions of different wave types and in situ generation of Rossby waves'. In: *Journal of the Atmospheric Sciences* 75.10, pp. 3613–3633.

Schoeberl, Mark R et al. (1992). 'The structure of the polar vortex'. In: *Journal of Geophysical Research: Atmospheres* 97.D8, pp. 7859–7882.

Smith, Anne K (1996). 'Longitudinal variations in mesospheric winds: Evidence for gravity wave filtering by planetary waves'. In: *Journal of Atmospheric Sciences* 53.8, pp. 1156–1173.

Stratosphere-Troposhere monitoring (n.d.). https://www.cpc.ncep.noaa.gov/products/stratosphere/strat-trop/.

Wang, L et al. (2020). 'What chance of a sudden stratospheric warming in the southern hemisphere?' In: *Environmental Research Letters* 15.10, p. 104038.

Whiteway, James A, Allan I Carswell and William E Ward (1995). 'Mesospheric temperature inversions with overlying nearly adiabatic lapse rate: An indication of a well-mixed turbulent layer'. In: *Geophysical Research Letters* 22.10, pp. 1201–1204.

Wit, Rosmarie J de (2015). 'Quantifying the influence of the stratosphere on the mesosphere and lower thermasphere'. In.

Appendix

Table 1: Months with corresponding day numbers for better understanding the plots.

Month	Day numbers
January	1-31
February	32-59
March	60-90
April	91-120
May	121-151
June	152-181
July	182-212
August	213-243
September	244-273
October	274-304
November	305-334
December	335-365

Table 2: Altitudes in km corresponding with the height model.

Height model	Altitude in km
0	18,4 km
2	24,8 km
4	32,9 km
6	41 km
8	50,3 km
10	60 km
12	69,7 km
14	78,8 km
16	86,9 km
17	91,6 km

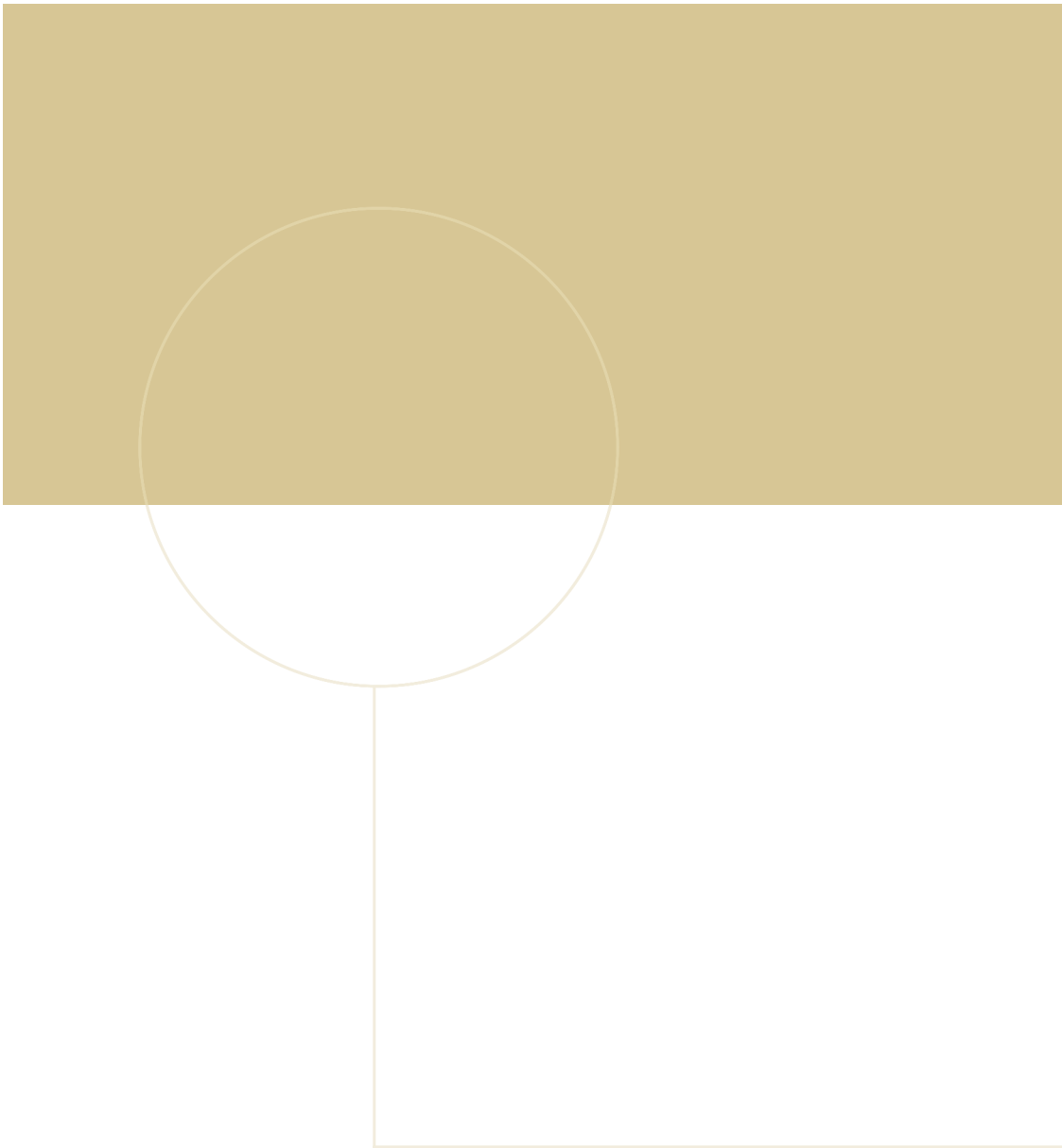

NTNU

Kunnskap for en bedre verden